Received: 21 November 2023 | Revised: 10 January 2024 | Accepted: 29 January 2024

DOI: 10.1002/pro.4925

RESEARCH NOTE

An intein-based biosensor to measure protein stability in vivo

Ahyun Son[1] | **John S. Smetana**[2] | **Scott Horowitz**[1] | **Christopher W. Lennon**[2]

[1]Department of Chemistry & Biochemistry, Knoebel Institute for Healthy Aging, University of Denver, Denver, Colorado, USA

[2]Department of Biological Sciences, Murray State University, Murray, Kentucky, USA

Correspondence
Christopher W. Lennon, Department of Biological Sciences, Murray State University, Murray, Kentucky 42071, USA.
Email: clennon1@murraystate.edu

Funding information
National Institutes of Health, Grant/Award Numbers: R35GM142442, P20GM103436, R15GM143662

Review Editor: Aitziber L. Cortajarena

Abstract

Biosensors to measure protein stability in vivo are valuable tools for a variety of applications. Previous work has demonstrated that a tripartite design, whereby a protein of interest (POI) is inserted within a reporter, can link POI stability to reporter activity. Inteins are translated within other proteins and excised in a self-mediated protein splicing reaction. Here, we developed a novel folding biosensor where a POI is inserted within an intein, which is subsequently translated within an antibiotic resistance marker. We showed that protein splicing is required for antibiotic resistance and that housing a stable POI within the intein, compared to an unstable variant, results in a 100,000-fold difference in survival. Further, using a fluorescent protein that matures slowly as the POI, we developed a reporter with two simultaneous readouts for protein folding. Finally, we showed that co-expression of GroEL can significantly increase the activity of both reporters, further verifying that protein folding factors can act on the POI in the biosensor. As a whole, our work provides a new twist on the traditional tripartite approach to measuring protein stability in vivo.

KEYWORDS

biosensor, chaperone, intein, protein folding, protein splicing

1 | INTRODUCTION

Protein folding is central to all biological processes, and protein misfolding is directly responsible for a variety of human diseases (Clausen et al., 2019). Biosensors for monitoring and engineering improved protein stability in vivo have enormous industrial and medicinal applications. Several tripartite protein folding biosensors have been developed where a protein of interest (POI) is translated within a reporter. In this design, the activity of the reporter will be based on the level of POI stability, with higher reporter activity associated with higher POI stability (Lennon et al., 2015; Malik et al., 2014; Ren et al., 2021). While this design has proven effective, previous iterations required that the POI remain fused to the reporter, restricting reporter function even with a well-folded POI, as well as limiting the size of POI insertion.

Inteins (**in**tervening pro**teins**) are mobile genetic elements that are translated within protein coding sequences and removed through protein splicing (Wood et al., 2023). In the intein-mediated reaction, the flanking sequences, termed N- and C-exteins, are joined with a peptide bond to form the mature host protein (ligated exteins) while the intein is released (Figure 1a). In addition to other conserved intein sequences, two nucleophilic side chains, the first residue of the intein (1 position) and the first residue of the C-extein (+1

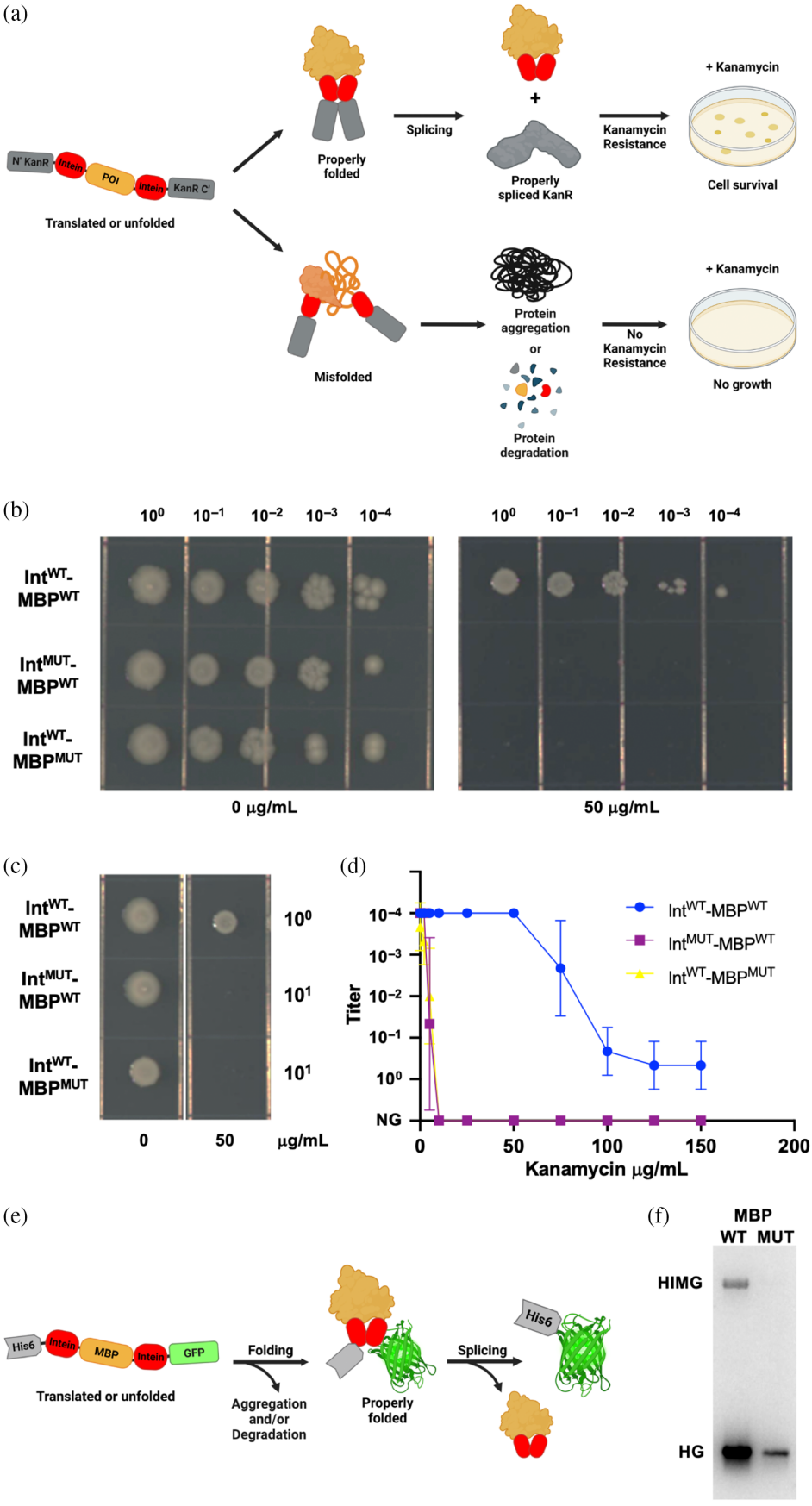

FIGURE 1 Intein-based biosensor links protein of interest (POI) folding to protein splicing. (a) Schematic of the intein-based protein folding biosensor. (b) Both splicing and POI stability are required for kanamycin resistance. The catalytically active Int^{WT} housing MBP^{WT} as a POI, but not a misfolding-prone MBP^{MUT}, provides robust resistance to kanamycin when inserted within the KanR protein. Protein splicing is required for kanamycin resistance, as the catalytically inactive Int^{MUT} housing MBP^{WT} as the POI provides no resistance to kanamycin under these conditions. (c) Growth of Int^{WT}-MBP^{WT} at a titer of 10^0 compared to Int^{MUT}-MBP^{WT} and Int^{WT}-MBP^{MUT} at a titer of 10^1 in the presence and absence of kanamycin. (d) Observed growth at the indicated titer over a range of kanamycin concentrations. (e) Cartoon of His-Int-MBP-GFP splicing reporter. (f) In-gel fluorescence of soluble protein following His-Int-MBP^{WT}-GFP and His-Int-MBP^{MUT}-GFP expression. In panel A, exteins, gray; intein, red; POI, orange. In panels (c), (d), and (e), cells were grown at 30°C for 72 h in Luria-Bertani plates containing 100 μg/mL of ampicillin and the indicated kanamycin concentration (right). Int^{MUT} indicates a C1A mutation. MBP^{MUT} indicates a G32D/I33P mutation. In panel C, NG indicates no growth. Error bars indicate the standard deviation from three independent experiments. In panel F, N-extein, black; intein, red; MBP, orange; C-extein, green. MBP, maltose binding protein.

position), drive the protein splicing reaction for class 1 inteins (Wood et al., 2023). This unique ability of inteins to specifically and controllably rearrange peptide bonds has garnered considerable interest in the engineering community, resulting in dozens of exciting applications (Sarmiento & Camarero, 2019; Wood et al., 2023). Here, we developed a novel intein-based tripartite protein folding sensor. By inserting a POI within an intein, our approach differs from previous systems in that if the POI folds properly, it does not remain fused to the reporter (Figure 1a). Additionally, using a slow-folding fluorescent POI, we showed that two readouts (antibiotic resistance and fluorescence) can be monitored within cells simultaneously.

2 | RESULTS

We hypothesized that the stability of a POI housed within an intein can influence the total amount of ligated exteins and thus reporter activity. By excising the POI upon proper folding, we anticipated a large enhancement of activity of the reporter protein compared to cases when the POI, even if properly folded, remains fused to the reporter protein (Figure 1b). To experimentally test this hypothesis, we chose maltose binding protein (MBP) as the POI and inserted it within the Homing Endonuclease (HEN) loop of the *Pyrococcus horikoshii* RadA (RadA-I). This loop, located between conserved splicing blocks, formally housed a HEN domain for intein mobility at the DNA level that has been lost during evolution. From an engineering perspective, the HEN loops of other inteins have been shown to accommodate foreign protein insertion (Buskirk et al., 2004; Ramsden et al., 2011; Skretas & Wood, 2005), and it was recently demonstrated that RadA-I can house the fluorescent protein ZsGreen and retain splicing activity (Heiden et al., 2022). This intein was also chosen as its splicing is particularly fast and accurate within several extein contexts (Ellilä et al., 2011; Oeemig et al., 2012; Topilina et al., 2015; Lennon et al., 2016), which is ideal as efficient self-removal should occur quickly if the intein folds properly.

We sought to first establish that a RadA-I-POI fusion inserted within KanR (aminoglycoside O-phosphotransferase APH(3′)-Ia; NCBI reference sequence WP_000018329.1) could retain kanamycin resistance. For an initial test POI, we inserted the intein-MBP fusion between residues 153 and 154 of KanR (KanR-I-I^{WT}-MBP^{WT}) with Ser154 of KanR acting as the +1 nucleophile (Figure 1a). This insertion position within KanR was chosen as we previously found that for another intein, DnaB1 from *Mycobacterium smegmatis*, protein splicing was required for kanamycin resistance in this position (Woods et al., 2020). Using quantitative spot titers in *E. coli*, we found that KanR-RadA-I^{WT}-MBP^{WT} provides resistance to 50 μg/mL kanamycin at 30°C (Figure 1c). Next, we determined whether splicing was required for resistance. To inhibit splicing, the first residue of the intein, a catalytic cysteine (Figure 1a), was mutated to alanine (KanR-RadA-I^{MUT}-MBP^{WT}). While robust growth was observed for KanR-RadA-I^{WT}-MBP^{WT}, we found no resistance with KanR-RadA-I^{MUT}-MBP^{WT} at 50 μg/mL kanamycin (Figure 1b).

We next tested the effect of a destabilizing mutation in MBP on kanamycin resistance. Previous work has shown that the MBP variant G32D/I33P (referred to as MBP^{MUT}) is aggregation-prone and has been used within other folding sensors (Lennon et al., 2015; Ren et al., 2021). We found that *E. coli* expressing KanR-RadA-I^{WT}-MBP^{MUT}, similar to KanR-RadA-I^{C1A}-MBP^{WT}, provides no resistance to 50 μg/mL kanamycin (Figure 1b). We reasoned that spotting a higher titer of cells may allow for either KanR-RadA-I^{MUT}-MBP^{WT} or KanR-RadA-I^{WT}-MBP^{MUT} to survive at 50 μg/mL kanamycin. However, even at a titer of 10^1 OD_{600}, no survival is observed (Figure 1c). This indicates an enormous dynamic range for our biosensor, with at least a 100,000-fold difference in survival at 50 μg/mL kanamycin between WT and G32D/I33P MBP.

We next examined resistance at kanamycin concentrations of 0, 2, 5, 10, 25, 50, 75, 100, 125, and 150 μg/mL (Figure 1d). Growth of KanR-RadA-I^{WT}-MBP^{WT} is observed at all concentrations tested, with a reduction at concentrations above 50 μg/mL. For both KanR-RadA-I^{MUT}-MBP^{WT} and KanR-RadA-I^{WT}-MBP^{MUT}, no growth is observed above 5 μg/mL kanamycin at any titer. In all cases, equal growth was observed in the absence of kanamycin (Figure 1b–d), fusion proteins were constitutively expressed from the same vector, and codons were optimized for *E. coli* expression, so it is unlikely that differences in translation would account for the 100,000-fold difference in survival between KanR-RadA-I^{WT}-MBP^{WT} and KanR-RadA-I^{WT}-MBP^{MUT}. These results demonstrate that the stability of a POI within an intein drastically alters intein activity, supporting the viability of our intein-based protein folding biosensor.

We next sought to examine the stability of our intein-MBP fusions by directly measuring soluble protein levels using a construct with a His-tag as the N-extein and GFP as the C-extein (Figure 1e). The fusion protein was expressed in *E. coli* and soluble GFP-containing products were visualized immediately following expression using in-gel fluorescence (Weinberger II & Lennon, 2021). Consistent with our observations with KanR, we observe substantially more ligated exteins with MBP^{WT} compared to MBP^{MUT} (Figure 1f; His-GFP). Further, these results

suggest that the MBP^{MUT} fusion protein either aggregates or is degraded quickly following translation as an unspliced precursor (Figure 1f; His-Int-MBP-GFP). These results demonstrate that the stability of a POI within an intein can drastically change the amount of ligated exteins produced, supporting the viability of our intein-based protein folding biosensor.

We then sought to test whether this intein-based folding biosensor strategy could be used to test the roles of protein folding modulators within the cell. To test this possibility, we employed a fluorescent protein, TagRFP675, as the POI. Similar to many other fluorescent proteins, TagRFP675 exhibits a slow maturation time (Balleza et al., 2018), resulting in kinetically trapped intermediates and poor folding in *E. coli* (Son et al., 2023). With the assistance of molecular chaperones, such as GroEL, TagRFP675 can overcome kinetic barriers to fold properly in *E. coli* (Son et al., 2023). Therefore, we used TagRFP675 to further investigate whether the reporter activity of the intein biosensor is correlated with the folding status of POI in the presence or absence of GroEL (Figure 2). Likely due to the dual expression vector system for POI and GroEL, which has two different antibiotic resistances as selective markers, as well as increased temperature from 30 to 37°C, the resulting resistance from the reporter was decreased from 50 to 20 μg/mL kanamycin. Without a co-expressed chaperone, we found that neither KanR-RadA-I^{WT}-MBP^{WT} nor KanR-RadA-I^{WT}-TagRFP675 confer resistance past 10^{-2} at 20 μg/mL kanamycin (Figure 2a). However, with the co-expression of GroEL, robust growth is observed for both KanR-RadA-I^{WT}-MBP^{WT} and KanR-RadA-I^{WT}-TagRFP675 (Figure 2a). These results indicate that with the assistance of GroEL, the survival of cells expressing KanR-RadA-I^{WT}-MBP^{WT} and KanR-RadA-I^{WT}-TagRFP675 is increased by 1000- and 10,000-fold,

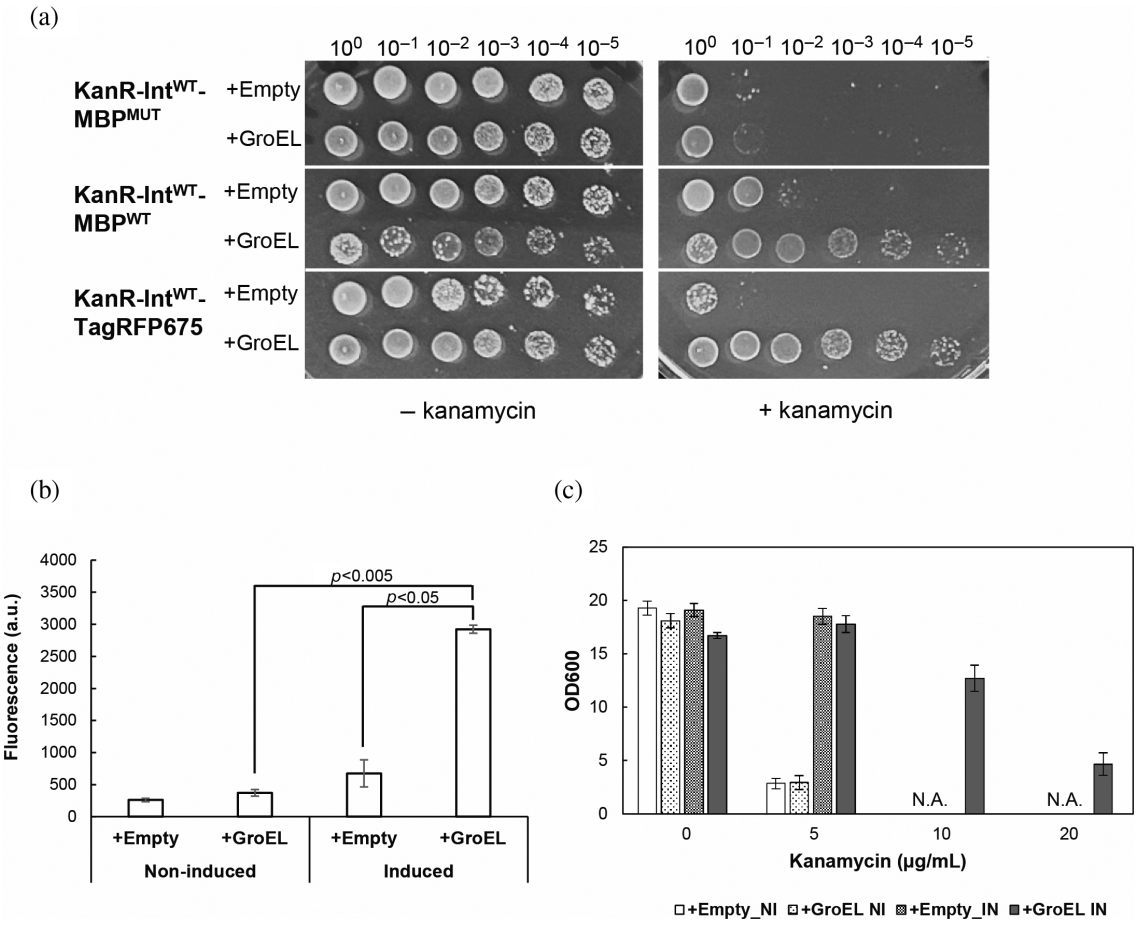

FIGURE 2 Intein biosensor detects protein folding and stability. (a) Spot titer assay of MBP^{MUT}, MBP^{WT}, and TagRFP675 in the presence or absence of a molecular chaperone, GroEL. Plates labeled as + kanamycin (right) contain 20 μg/mL of kanamycin. (b) Fluorescence assay of TagRFP675 with 5 μg/mL of kanamycin. (c) OD_{600} measurements for each sample with various concentrations of kanamycin (0, 5, 10, 20 μg/mL). The error bars shown in (b) and (c) are the mean ± SE ($n = 3$) of technical triplicates. Significant differences between two groups (t-test) are denoted by $p < 0.005$ and 0.05. All experiments shown here were performed at 37°C and repeated more than 3 times in triplicate. NI and IN indicate Noninduced and induced, respectively.

respectively. Unexpectedly, co-expression of GroEL does not increase survival of KanR-RadA-I^{WT}-MBP^{MUT} (Figure 2a), likely due to the highly aggregation-prone characteristics of the mutant MBP (Figure 1f).

To determine whether higher kanamycin resistance is correlated with higher levels of folded TagRFP675, we measured its fluorescence in *E. coli* with and without a co-expressed chaperone (Figure 2b). In the presence of induced GroEL, TagRFP675 showed considerably higher fluorescence, consistent with the increased kanamycin resistance (Figure 2c). Taken together, these data further support that our intein biosensor enables the detection of proper folding and stability of POIs. Additionally, our results demonstrate that both antibiotic resistance and fluorescence can be measured from our KanR-RadA-I^{WT}-TagRFP675 folding biosensor, allowing for two simultaneous readouts of protein folding.

3 | DISCUSSION

In this study, we examined the utility of including inteins in the design of protein folding biosensors in cells. By employing the tripartite intein-based protein folding biosensor (Figure 1b), we demonstrated that the stability of a POI strongly influences survival in the presence of kanamycin (Figure 1c). Furthermore, this intein-based biosensor could be used to examine the roles of protein folding modulators, such as molecular chaperones, in enhancing protein folding of a POI in cells (Figure 2). Additionally, by using a fluorescent protein as the POI, we also engineered a dual folding sensor with both fluorescence and antibiotic resistance linked to POI folding. Together, these results underscore the potential of inteins as an effective tool to analyze the folding dynamics of various POIs in cellular contexts.

It is not possible at this time to directly compare our intein-based reporter to previous tripartite designs for several reasons. First, our splicing-dependent reporter was designed to block kanamycin resistance prior to intein-POI removal. Conversely, previous tripartite designs were designed to permit antibiotic resistance while accommodating an internal POI. While a previous tripartite system using kanamycin resistance has been reported, it utilizes a different KanR protein that is only 32% conserved to the KanR protein used in this work, and neither MBP nor TagRFP675 were tested as POIs (Malik et al., 2014). The MBP^{WT} and MBP^{MUT} used in this work as POIs were previously inserted within another antibiotic resistance protein, β-lactamase (Lennon et al., 2015). In that work, MBP^{WT} survived ~100-fold better than MBP^{MUT} at 100 mg/mL ampicillin (Lennon et al., 2015). While we observe ~100,000-fold difference in survival between the MBP^{WT} and MBP^{MUT}, future work will be necessary to directly compare the traditional tripartite system to our intein-based approach.

It is challenging to select an appropriate model organism that is suitable for the expression of target POIs. Our biosensor system, therefore, could provide a versatile platform applicable for choosing the most suitable cellular model for efficient POI production. As intein-based tools have been developed for use in several prokaryotic and eukaryotic systems (Sarmiento & Camarero, 2019; Wang et al., 2022; Wood et al., 2023), our approach should be applicable to a wide range of cellular environments. Additionally, as the intein-POI does not remain fused to the reporter, and the only strict requirement for protein splicing is the presence of a Cys, Ser, or Thr residue immediately following the intein, our approach could hypothetically be used to link protein stability to any in vivo readout, including fluorescence (e.g., GFP), auxotrophic markers (e.g., URA3), and colorimetric signals (e.g., β-galactosidase) to name a few. Moreover, our approach opens new avenues for exploring the effects of various protein folding modulators, including small molecules and molecular chaperones, to enhance the productivity of POIs. Overall, our biosensor system not only contributes to advancing our understanding of protein folding within cellular environments but also offers practical applications in optimizing protein production strategies.

4 | MATERIALS AND METHODS

4.1 | Construction of expression vectors and nucleic acid sourcing

Strains and plasmids are listed in Tables 1 and 2, respectively. Plasmids pKanR-RadA-I^{WT}-MBP^{WT}, pKanR-RadA-I^{C1A}-MBP^{WT}, pKanR-RadA-I^{WT}-MBP$^{G32D/I33P}$, and pKanR-RadA-I^{WT}-TagRFP675 were prepared by

TABLE 1 Bacterial strains.

Strains	Genotype	References
BL21 (DE3)	*fhuA2 [lon] ompT gal (λ DE3) [dcm] ΔhsdS λ DE3 = λ sBamHIo ΔEcoRI-B int::(lacI::PlacUV5::T7 gene1) i21 Δnin5*	New England Biolabs
NEB5α	*Φ80 Δ(lacZ)M15 Δ(argF-lacZ) recA1 endA1 hsdR17 fhuA2*	New England Biolabs
MC4100 (DE3)	*Δ(argF-lacZ) U169 araD139 rpsLS50 reLAl deoCI ptsF25 rpsR flbB301 (DE3)*	Casadaban, 1976

TABLE 2 Plasmids.

Strain number	Plasmid1		Plasmid2		Strains	References
CWL547	His-Int-MBP^{MUT}-GFP	KnR			BL21(DE3)	This study
CWL551	His-Int-MBP^{WT}-GFP	KnR			BL21(DE3)	This study
CWL599	KanR-Int^{WT}-MBP^{MUT}	ApR			NEB5α	This study
CWL600	KanR-Int^{WT}-MBP^{WT}	ApR			NEB5α	This study
CWL640	KanR-Int^{MUT}-MBP^{WT}	ApR			NEB5α	This study
AS917	KanR-Int^{WT}-MBP^{MUT}	ApR	pBAD33mut-Empty	CmR	MC4100(DE3)	This study
AS923	KanR-Int^{WT}-MBP^{MUT}	ApR	pBAD33-GroEL	CmR	MC4100(DE3)	This study
AS925	KanR-Int^{WT}-MBP^{WT}	ApR	pBAD33mut-Empty	CmR	MC4100(DE3)	This study
AS931	KanR-Int^{WT}-MBP^{WT}	ApR	pBAD33-GroEL	CmR	MC4100(DE3)	This study
AS933	KanR-Int^{WT}-TagRFP675	ApR	pBAD33mut-Empty	CmR	MC4100(DE3)	This study
AS939	KanR-Int^{WT}-TagRFP675	ApR	pBAD33-GroEL	CmR	MC4100(DE3)	This study

Genscript from a pUC4K background (Vieira & Messing, 1982). Plasmid pUC4K has both β-lactamase and KanR for resistance to ampicillin and kanamycin, respectively. KanR was interrupted by the intein fusions between residues 153 and 154, with Serine 154 acting as the +1 nucleophile. *E. coli* MBP (residues 27–396) or TagRFP675 (Merzlyak et al., 2007) was inserted between residues 126 and 127 of the RadA-I. Short Gly-Ser linkers were added between the intein and TagRFP675. Plasmids pHis-Int^{WT}-MBP^{WT}-GFP and pHis-Int^{WT}-MBP^{MUT}-GFP were prepared by Genscript from a pET28b(+).

The pBAD33 vector was used to construct pBAD33-GroEL and pBAD33mut-empty. The GroEL gene was obtained from the *E.coli* genome by PCR. pBAD33-GroEL was constructed using the SacI and HindIII sites on the multiple cloning site (MCS) of pBAD33. pBAD33mut-Empty vector was obtained by changing the MCS of the pBAD33 vector into SacI and SpeI sites using MluI and BglII restriction enzymes.

4.2 | Spot titer assays

For experiments without co-expression of GroEL (or empty pBAD control), *E. coli* (NEB5a) constitutively expressing KanR fusions were grown for ~20 h at 37°C in Luria-Bertani (LB) medium with 100 mg/mL ampicillin (for plasmid maintenance). Cells were next diluted to OD_{600} values of 10,[1] 10^0, 10^{-1}, 10^{-2}, 10^{-3}, and 10^{-4} in LB and 1.25 μL of each dilution was spotted on LB agar containing 100 μg/mL ampicillin and 0–150 μg/mL kanamycin and grown at 30°C for 3 days. Cell titers and kanamycin concentrations are indicated in Figure 1 and its legend.

For experiments with co-expression of GroEL (or empty pBAD control), each resulting expression vector of biosensor protein, KanR-Int^{WT}-MBP^{MUT}, KanR-Int^{WT}-MBP^{WT}, and KanR-Int^{WT}-TagRFP675, and pBAD33-GroEL or pBAD33mut-Empty were co-transformed into the *E.coli* strain MC4100(DE3) by heat shock. Each transformant was inoculated into 3 mL of LB medium containing 200 μg/mL of ampicillin and 35 μg/mL of chloramphenicol and incubated at 37°C overnight with vigorous shaking. The next day, 200 μL of each start culture was transferred into fresh 3 mL of LB medium with the same concentrations of antibiotics used above. When the OD_{600} reaches >0.5–0.6, 0.1% *L*-Arabinose was added to induce the expression of GroEL for 2 h. The OD_{600} of each sample was measured and normalized to 1.0 OD_{600} with 1X phosphate-buffered saline (PBS) (pH 7.4) for further spot titer and fluorescence assays. To perform the spot titer assay, each 1.0 OD_{600} of sample was serially (10-fold) diluted to 10^{-5} OD_{600} with 1X PBS (pH 7.4) on a nonbinding 96-well plate (Greiner Bio-One, 655904). LB plates containing 0.2% *L*-Arabinose, chloramphenicol (35 μg/mL), and various concentrations of kanamycin (0, 5, 10, and 20 μg/mL) were used. To compare the expression of GroEL, noninducing LB plates containing the same amount of antibiotic(s) except 0.2% *L*-Arabinose were used. The serial dilutions of noninduced or induced samples were spotted (5 μL) on the LB plates and incubated at 37°C overnight (16–20 h) or at room temperature for 2 days. All spot titer assays were performed at least 3 times for consistency.

4.3 | His-Int-MBP-GFP expression and in-gel fluorescence

BL21(DE3) *E. coli* containing either pHis-Int-MBP^{WT}-GFP or pHis-Int-MBP^{MUT}-GFP was grown to mid-log phase at 37°C in LB with 50 μg/mL of kanamycin (for plasmid maintenance), and protein expression was induced by the addition of isopropyl ß-D-1-

thiogalactopyranoside (GoldBio) to a final concentration of 1 mM. Following induction, His-Int-MBP^{WT}-GFP or His-Int-MBP^{MUT}-GFP was expressed for 3 hours at 37°C, and cells were pelleted by centrifugation, resuspended in 50 mM Tris-HCl pH 8.0, 10% glycerol, and lysed by sonication. Insoluble material was removed by centrifugation, soluble protein was resolved by semi-native PAGE, and fluorescent proteins were visualized as described (Weinberger II & Lennon, 2021) using an Amersham Imager 600 (GE Healthcare).

4.4 | Fluorescence assays of TagRFP675

For the fluorescence assay, 50 µL of each 1.0 OD_{600} sample were spread on LB plates with the same amount of antibiotic(s) explained above and incubated at 37°C overnight (16–20 hours). The next day, entire cells from each plate were scraped in 1× PBS (pH 7.4), harvested by centrifugation at 10,000 g for 1 min, and resuspended with 1 mL of 1× PBS (pH 7.4). Because the cells co-expressed with the empty vector only provide resistance to 5 µg/mL kanamycin and failed to survive on the plates containing more than 10 µg/mL of kanamycin, the fluorescence of cells from plates with 5 µg/mL of kanamycin was measured to compare the fluorescence between the empty vector and GroEL expression. Cell growth (OD_{600}) was measured with a spectrophotometer (GENESYS™ 10S UV–Vis Spectrophotometers, Thermo Scientific). Cells were then diluted to 1 OD_{600} with 1× PBS (pH 7.4) for further fluorescence assays. Fluorescence emission of TagRFP675 (at 675 nm) was measured upon excitation at 598 nm using a microplate reader (Infinite M200 Pro, Tecan) and a black 96-well plate (Corning Black NBS 3991). All fluorescence assays were performed in triplicate at least 3 times.

AUTHOR CONTRIBUTIONS

Christopher Lennon: Conceptualization; project administration; supervision; methodology; funding acquisition; writing – review and editing; writing – original draft; formal analysis; data curation; visualization. **Ahyun Son:** Methodology; investigation; writing – review and editing; writing – original draft; visualization; formal analysis; data curation. **John S. Smetana:** Writing – review and editing; investigation; methodology. **Scott Horowitz:** Supervision; funding acquisition; writing – original draft; writing – review and editing; methodology.

ACKNOWLEDGMENTS

We acknowledge support from the National Institutes of Health grants R15GM143662 and P20GM103436 (via KY INBRE) to CWL and NIH R35GM142442 to SH.

CONFLICT OF INTEREST STATEMENT

The authors declare no conflict of interest.

DATA AVAILABILITY STATEMENT

All data that support the findings of this study are available upon request from the corresponding author.

ORCID

Ahyun Son https://orcid.org/0000-0002-7979-0409
Scott Horowitz https://orcid.org/0000-0002-1148-0105
Christopher W. Lennon https://orcid.org/0000-0001-9413-180X

REFERENCES

Balleza E, Kim JM, Cluzel P. Systematic characterization of maturation time of fluorescent proteins in living cells. Nat Methods. 2018;15:47–51.

Buskirk AR, Ong Y-C, Gartner ZJ, Liu DR. Directed evolution of ligand dependence: small-molecule-activated protein splicing. Proc Natl Acad Sci U S A. 2004;101:10505–10.

Casadaban MJ. Transposition and fusion of the lac genes to selected promoters in Escherichia coli using bacteriophage lambda and Mu. J Mol Biol. 1976;104:541–55.

Clausen L, Abildgaard AB, Gersing SK, Stein A, Lindorff-Larsen K, Hartmann-Petersen R. Protein stability and degradation in health and disease. Adv Protein Chem Struct Biol. 2019;114:61–83.

Ellilä S, Jurvansuu JM, Iwaï H. Evaluation and comparison of protein splicing by exogenous inteins with foreign exteins in *Escherichia coli*. FEBS Lett. 2011;585:3471–7.

Heiden B, Mühlberger E, Lennon CW, Hume AJ. Labeling Ebola virus with a self-splicing fluorescent reporter. Microorganisms. 2022;10:2110.

Lennon CW, Stanger M, Belfort M. Protein splicing of a recombinase intein induced by ssDNA and DNA damage. Genes Dev. 2016;30:2663–8.

Lennon CW, Thamsen M, Friman ET, Cacciaglia A, Sachsenhauser V, Sorgenfrei FA, et al. Folding optimization in vivo uncovers new chaperones. J Mol Biol. 2015;427:2983–94.

Malik A, Mueller-Schickert A, Bardwell JCA. Cytosolic selection systems to study protein stability. J Bacteriol. 2014;196:4333–43.

Merzlyak EM, Goedhart J, Shcherbo D, Bulina ME, Shcheglov AS, Fradkov AF, et al. Bright monomeric red fluorescent protein with an extended fluorescence lifetime. Nat Methods. 2007;4:555–7.

Oeemig JS, Zhou D, Kajander T, Wlodawer A, Iwaï H. NMR and crystal structures of the Pyrococcus horikoshii RadA intein guide a strategy for engineering a highly efficient and promiscuous intein. J Mol Biol. 2012;421:85–99.

Ramsden R, Arms L, Davis TN, Muller EG. An intein with genetically selectable markers provides a new approach to internally label proteins with GFP. BMC Biotechnol. 2011;11:71.

Ren C, Wen X, Mencius J, Quan S. An enzyme-based biosensor for monitoring and engineering protein stability in vivo. Proc Natl Acad Sci U S A. 2021;118:e2101618118.

Sarmiento C, Camarero JA. Biotechnological applications of protein splicing. CPPS. 2019;20:408–24.

Skretas G, Wood DW. Regulation of protein activity with small-molecule-controlled inteins. Protein Sci. 2005;14:523–32.

Son A, Huizar Cabral V, Huang Z, Litberg TJ, Horowitz S. G-quadruplexes rescuing protein folding. Proc Natl Acad Sci U S A. 2023;120:e2216308120.

Topilina NI, Novikova O, Stanger M, Banavali NK, Belfort M. Post-translational environmental switch of RadA activity by extein-intein interactions in protein splicing. Nucleic Acids Res. 2015; 43:6631–48.

Vieira J, Messing J. The pUC plasmids, an M13mp7-derived system for insertion mutagenesis and sequencing with synthetic universal primers. Gene. 1982;19:259–68.

Wang H, Wang L, Zhong B, Dai Z. Protein splicing of inteins: a powerful tool in synthetic biology. Front Bioeng Biotechnol. 2022;10:810180.

Weinberger J II, Lennon CW. Monitoring protein splicing using in-gel fluorescence immediately following SDS-PAGE. Bio Protoc. 2021;11:e4121.

Wood DW, Belfort M, Lennon CW. Inteins—mechanism of protein splicing, emerging regulatory roles, and applications in protein engineering. Front Microbiol. 2023;14:1305848.

Woods D, Vangaveti S, Egbanum I, Sweeney AM, Li Z, Bacot-Davis V, et al. Conditional DnaB protein splicing is reversibly inhibited by zinc in mycobacteria. mBio. 2020;11:e01403-20.

How to cite this article: Son A, Smetana JS, Horowitz S, Lennon CW. An intein-based biosensor to measure protein stability in vivo. Protein Science. 2024;33(3):e4925. https://doi.org/10.1002/pro.4925